



HAL
open science

First evidence of rock wall permafrost in the Pyrenees (Vignemale peak, 3,298 m a.s.l., 42°46'16 N/0°08'33 W)

Ibai Rico, Florence Magnin, Juan Ignacio López Moreno, Enrique Serrano,
Esteban Alonso-González, Jesús Revuelto, Lara Hughes-Allen, Manuel
Gómez-Lende

► To cite this version:

Ibai Rico, Florence Magnin, Juan Ignacio López Moreno, Enrique Serrano, Esteban Alonso-González, et al. First evidence of rock wall permafrost in the Pyrenees (Vignemale peak, 3,298 m a.s.l., 42°46'16 N/0°08'33 W). *Permafrost and Periglacial Processes*, 2021, 32 (4), pp.673-680. 10.1002/ppp.2130 . hal-03024120

HAL Id: hal-03024120

<https://hal.science/hal-03024120v1>

Submitted on 25 Nov 2020

HAL is a multi-disciplinary open access archive for the deposit and dissemination of scientific research documents, whether they are published or not. The documents may come from teaching and research institutions in France or abroad, or from public or private research centers.

L'archive ouverte pluridisciplinaire **HAL**, est destinée au dépôt et à la diffusion de documents scientifiques de niveau recherche, publiés ou non, émanant des établissements d'enseignement et de recherche français ou étrangers, des laboratoires publics ou privés.

1 **First evidence of rock wall permafrost in the Pyrenees (Southwestern Europe, 42°N)**

2 Ibai Rico¹, Florence Magnin², Juan Ignacio López Moreno³, Enrique Serrano⁴, Esteban
3 Alonso-González³, Jesús Revuelto³, Lara Hughes-Allen⁵, Manuel Gómez-Lende⁶.

4 1 Department of Geography, Prehistory and Archaeology. University of the Basque
5 Country. Vitoria-Gasteiz, Spain.

6 2 CNRS – Université Savoie Mont-Blanc. Campus scientifique USMB. Le Bourget-
7 du-lac, France.

8 3 Pyrenean Institute of Ecology. Consejo Superior de Investigaciones Científicas.
9 Zaragoza, Spain.

10 4 Department of Geography. University of Valladolid. Valladolid, Spain.

11 5 Université Paris-Saclay, CNRS, GEOPS, 91405, Orsay, France

12 6 PANGEA Department of Geography. University of Valladolid. Valladolid, Spain.

13

14 **Abstract**

15 Permafrost is an important component of the Pyrenean high mountains, including a wide
16 range of geomorphological cryogenic processes. While there has been an increase in
17 frozen ground studies in the Pyrenees, there are no specific studies about rock wall
18 permafrost, its presence, distribution, regime or historical evolution. This work combines
19 measured rock surface temperatures along an elevation profile of the north face wall of
20 the Vignemale peak (main divide of Central Pyrenees) and temperature modelling for this
21 mountain, in order to ascertain the presence of permafrost and to analyze its evolution
22 since the mid-XX century. Results reveal that the entire rock face was affected by warm
23 permafrost (> -2°C), as low as 2600 m a.s.l from 1961 to 1990. By 1981-2010, the limit
24 of close to 0°C permafrost rose to around 2800 m a.s.l and it has reached 3000 m a.s.l by
25 present day. Conditions permit cold (< -2°C) permafrost on north faces above 3100-3200
26 m a.s.l. The large expansion of warm permafrost suggests an imminent disappearance of
27 permafrost in the Vignemale and in most of the peaks of the Pyrenees.

28 **Key words:** Rock wall permafrost, temperature measurements, temperature modelling,
29 climate warming, Vignemale peak, Pyrenees.

30 **1 Introduction**

31 High mountain permafrost plays an important role in the precipitation of rock falls and
32 other mass movements and has become an emerging field of research over the past decade
33 ¹⁻³. Rock wall permafrost distribution is mainly determined by elevation (air temperature)
34 and slope-shading (incoming short-wave solar radiation affected by cast shadows). These
35 permafrost areas are exceptionally sensitive to climate change because of the direct
36 contact with the atmosphere, relatively low ice content and multi-sided heat propagation
37 into sharp and complex topographies ⁴.

38 The Pyrenean high mountains occupy around 365 km² and hold 132 peaks over 3000
39 m a.s.l. Steep rock walls and north faces occupy a significant part of this environment
40 such as in the massifs of Balaitous, Monte Perdido or Aneto-Maladeta among others.

41 Studies have found that the lower limit of discontinuous permafrost in the region is around
42 2700 m a.s.l, ⁵⁻⁷ - which is generally at a higher elevation than other European mountain
43 ranges ⁸⁻¹⁰ - and continuous permafrost is only found above 3000 m a.s.l. However, there
44 is a paucity of comprehensive rock wall permafrost studies in one of the lowest-latitude
45 permafrost affected mountain ranges of the northern hemisphere ¹¹. The rapid degradation
46 of permafrost in this mountain range has the potential to trigger large slope and mass
47 wasting processes with important socio-economic impacts ⁵ as well as risks associated
48 with mountaineering activities ¹².

49 The main aims of this study are 1) to verify the presence or absence of permafrost in the
50 high-elevation north face of the Vignemale and 2) to reconstruct the historical evolution
51 and degradation pathways of rock wall permafrost in this north face.

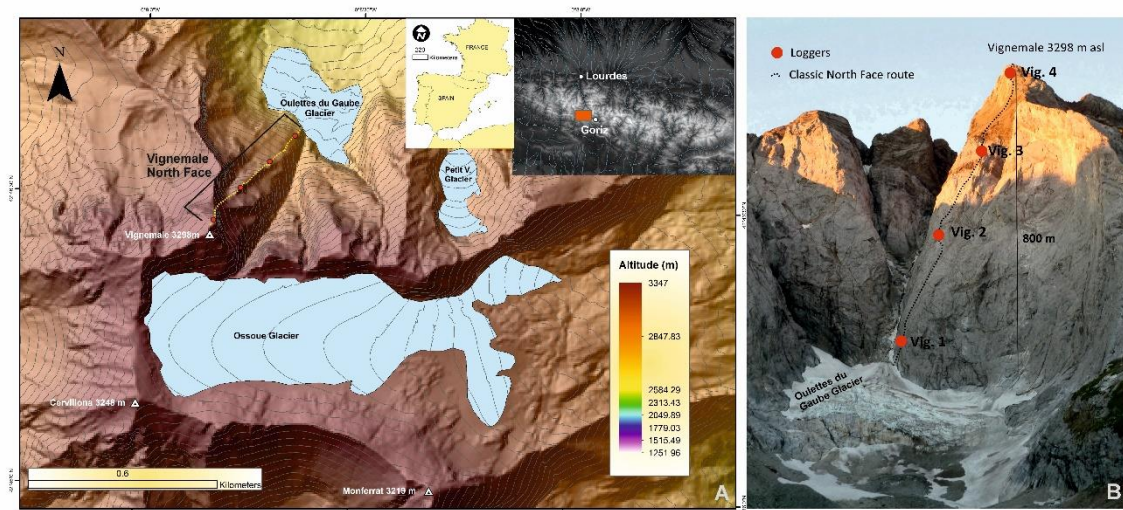
52 **2 Study Site**

53 The Vignemale Peak (3298 m a.s.l, 42°46'16" N / 0°08'33" W) is located in the Vignemale
54 massif (Pyrenees National Park, France; Fig. 1). A north-south oriented fault-system has
55 created strong relief asymmetries, generating a deep glacial valley towards the north,

56 where rock walls of more than 800 m of vertical difference define a unique alpine
57 landscape in this temperate mountain range. The north face of the Vignemale peak was
58 first climbed in 1933 by Henri Barrio and Robert Bellocq, establishing the present-day
59 route known as the North Face Classic route (D+, 800 m).

60 The Vignemale north face shapes the glacial cirque located at the uppermost section of
61 the Gaube valley. The wall experiences constant geodynamic processes including snow
62 avalanches during winter and spring and rockfalls in the summer season. Local mountain
63 guides and members of the Gendarmerie rescue team have reported an increase in rock
64 falls during the last decade ¹³.

65 In the Pyrenees, mean temperature has increased by 1.3 °C since 1955, with no significant
66 changes in precipitation ¹⁴, accelerating the shrinkage of remaining glaciers, which are
67 currently in a critical situation and likely to completely disappear ¹⁵⁻¹⁷. Mean annual
68 temperature recorded at the summit of nearby Midi de Bigorre peak (2877 m a.s.l.) -
69 0.13°C, very close to the 0°C isotherm. No direct observations of precipitation are
70 available for the study area, but annual precipitation is estimated to exceed 2,000 mm yr⁻¹
71 ¹⁸. Most of the Vignemale massif is covered by snow for seven to nine months (from
72 October-November to the following late May-early July), although climate warming has
73 reduced the duration of cover ¹⁹. However, the north face of the Vignemale peak remains
74 mostly free of snow due to the steep (mean slope of 70°) topography of the alpine rock
75 walls.



76

77 **Figure 1.** Study area (A) and the Vignemale North Face with the location of temperature
 78 loggers (B).

79 **3 Material and Methods**

80 **3.1 Rock Surface Temperature time series**

81 In September 2013, we equipped the north face of the Vignemale (3298 m a.s.l.) with
 82 four temperature loggers following an altitudinal profile spanning 2617-3196 m a.s.l.
 83 (Tab.1). We placed Ibutton DS1923 temperature and humidity loggers at approximately
 84 5 cm depth and sealed the borehole with synthetic silicone. These loggers have a
 85 temperature measuring range from -20 to + 85 °C and a technical precision of ± 0.5 °C²⁰.
 86 Temperature data were recorded every four hours (Tab. 1). Sensors were replaced in
 87 September 2014 and finally retrieved in October 2016.

Logger name	Vig_1	Vig_2	Vig_3	Vig_4
Time frame 1 (dd.mm.yyyy)	08/09/2013 - 26/07/2014	08/09/2013 - 26/07/2014	08/09/2013 - 25/04/2014	08/09/2013 - 25/04/2014
Time frame 2	-	-	02/09/2014 -1 02/04/2016	02/09/2014 - 02/04/2016
Coordinates	42° 46.604'N 0° 8.596'W	42° 46.551'N 0° 8.697'W	42° 46.511'N 0° 8.770'W	42° 46.470'N 0° 8.850'W
Elevation	2617 m a.s.l	2803 m a.s.l	2983 m a.s.l	3196 m a.s.l
Aspect	NE (45°)	NE (45°)	NE (45°)	N (0°)

88

89 **Table 1.** *Operational time frame and description of location of the installed loggers.*

90 Loggers Vig_1, Vig_2, and Vig_3 were placed at a maximum elevation of 2983 m a.s.l
91 and below the elevation of the Ossoue glacier plateau on the opposite south side of the
92 massif. Vig_4 is located at 3196 m a.s.l on the summit ridge and well above the Ossoue
93 glacier plateau. The two lowest loggers (Vig_1 and Vig_2) registered data for 11 months
94 (failure due to exposure to extreme conditions) and the highest two sensors (Vig_3 and
95 Vig_3) covered 2.5 years including a gap of 1.5 months (Tab. 1; Fig. S1).

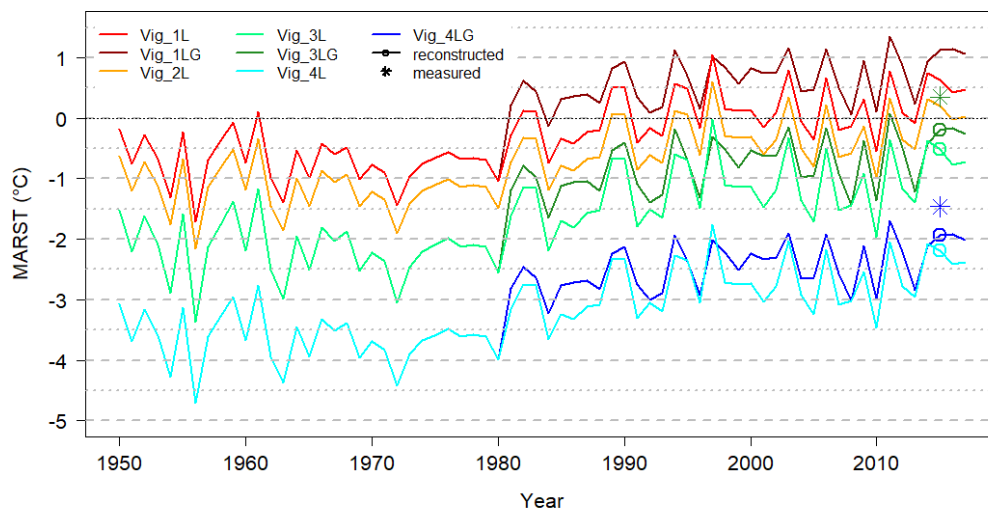
96 *1.1 Prediction of rock surface temperature evolution with air temperature*

97 In the absence or limited accumulation of debris or snow, rock surface temperature (RST)
98 is closely coupled with air temperature (AT), particularly on north faces where the effect
99 of incoming shortwave solar radiations is negligible. Therefore, it is possible to model
100 RST history based on AT time series ^{4,21}. These predictions can then be used to evaluate
101 whether past conditions were favorable to the formation of permafrost. We formulated
102 three linear regression models per sensor to predict RST time series using temperature
103 data from nearby Lourdes (Météo France 420 m a.s.l) and Goriz (2200 m a.s.l.) weather
104 stations (Tab.S2):

- 105 - *All year Lourdes*: calibrated with the Lourdes AT and all RST measurements:
- 106 - *Winter Lourdes*: calibrated with Lourdes AT from mid-September to mid-May and
107 corresponding RST
- 108 - *Summer Goriz*: calibrated with Goriz AT from mid-May to mid-September and
109 corresponding RST

110 The *Winter Lourdes* and *Summer Goriz* linear models were combined (hereafter called
111 the *Lourdes-Goriz (L-G)* regression) to predict year-round RST and better represent
112 measured RST during summer (Fig. S2). However, for Vig_2 the regression with Goriz
113 was insignificant (Tab. S2) and was thus ignored for the following data processing.

114 Summary statistics of models' errors at various time aggregations (daily, monthly, and
 115 annual) given in Table S3 show that bias between predicted and measured mean annual
 116 RST (MARST) is lower for Vig_3 and Vig_4 when considering the *Lourdes-Goriz*
 117 regression. Standard deviations for daily and monthly values are also improved.
 118 Two RST time series were formulated per logger for Vig_1, Vig_3 and Vig_4 using the
 119 *All year Lourdes* regression from 1950 to 2018 and the *Lourdes-Goriz* regression from
 120 July 1981 to 2018 (Fig. 2). For Vig_2, only one time series was formulated with the *All*
 121 *year Lourdes* regression (the regression with Goriz was insignificant). All RST time
 122 series began in 1950 and ended in 2018, except the times series predicted with the
 123 *Lourdes-Goriz* regression, which began in 1981 when the Goriz station started recording.
 124 Measured RST replaced reconstructed RST when available in each of these time series.



125
 126 **Figure 2.** Evolution of the mean annual RST as predicted with the different regressions.
 127 “L” after Vig_x is the time series reconstructed with Lourdes AT, while “LG” is the
 128 time series reconstructed with the Lourdes-Goriz regression. The “reconstructed” and
 129 “measured” symbols represent the mean annual rock surface temperature (MARST) for
 130 the full hydrological year that is available with measurements.

131 1.2 Thermal modelling

132 We use the CryoGRID2 model ²² to assess permafrost evolution and characteristics at
133 depth. We forced the top of the profile with the RST time series and at each time step, the
134 profile at time $n-1$ is used as an input for calculating the temperature profile at time n . We
135 applied a thermal conductivity of $2.5 \text{ W m}^{-1}\text{K}^{-1}$, which is a standard value for limestone
136 ²³ (main Vignemale massif's material). We ran simulations with different porosity values
137 to test the sensitivity of our model to this poorly known parameter: 1% and 5% along the
138 entire bedrock profile. While the former value is standard for compact limestone, the latter
139 accounts for bedding that could increase the bulk porosity. Similar characteristics are
140 considered for Vig_4 that lay in the Devonian schist combining carbonate and pelitic
141 rock.

142 The temperature-depth profile of alpine rock wall is partly controlled by lateral heat fluxes
143 resulting from variable energy balances between opposite faces ⁴. For Vig_1, Vig_2 and
144 Vig_3, no bottom heat flux was included in run simulations. However, Vig_4, the
145 opposite south slope corresponds to a gently inclined plateau that is approximately 200
146 m away and is suspected to have a significant influence on the near surface thermal
147 regime. In the absence of measurements on the south face (due to sensors failure), we
148 determined a bottom heat flux based on assumptions formulated from previous studies on
149 rock wall permafrost ^{21,24,25}. We thus perform several runs for Vig_4 accounting for no
150 basal heat flux and a heat flux corresponding to an 8°C difference with the opposite south
151 face (0.1 W. m^2) to provide a range of possible extreme values.

152 Before each simulation, the 10 first years predicted using the Lourdes regression (1950-
153 1960) were run to initialize the thermal profiles. The spatial resolution of the simulated
154 thermal profile was 0.1 m between the surface and 1 m depth, 0.2 m between 1 and 5 m
155 depth, 0.5 m between 5 and 10 m depth and 1 m down to 30 m depth.

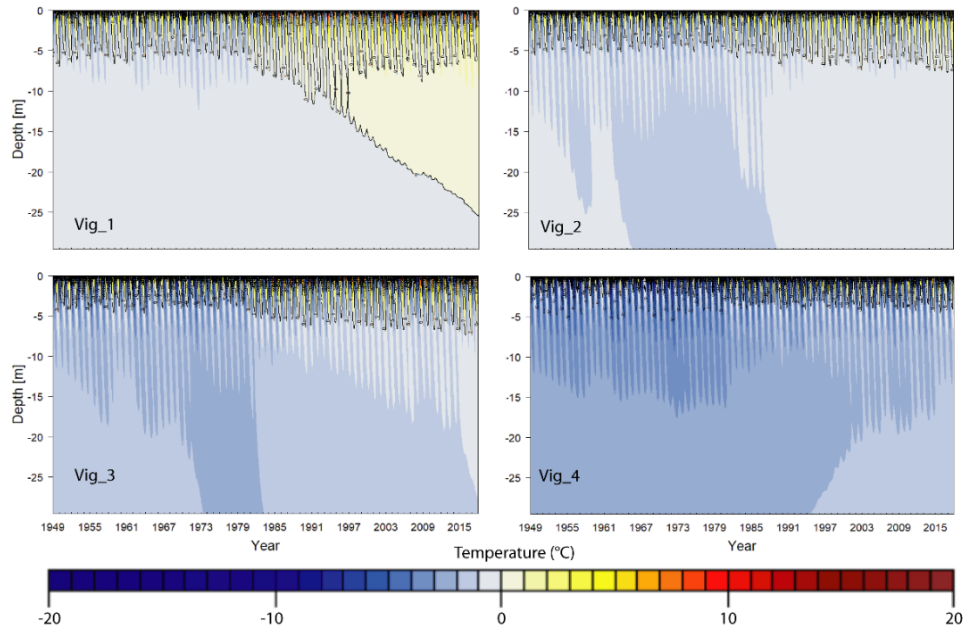
156 **2 Results**

157 2.1 *Permafrost evolution since the 1950s*

158 The predicted MARST for the period 1961-1990 shows that permafrost may have been
 159 present within the entire rock face and mostly characterized by warm permafrost ($> -2^{\circ}\text{C}$),
 160 except at the extreme elevations (above 3100 m a.s.l) where cold permafrost ($< -2^{\circ}\text{C}$) is
 161 suggested (Tab. 2; Fig. 3). At Vig_2 and Vig_3, heat transfer simulations suggest that the
 162 coldest conditions were between 1970-1980. During the period 1981-2010, predicted
 163 MARST suggests that permafrost was no longer present at Vig_1 and simulated
 164 temperature profiles show a deepening of positive temperature ($> 0^{\circ}\text{C}$) from the 2000s,
 165 reaching a depth of > 20 m at present (Fig. 3). However, simulations using higher ice
 166 content value (5% porosity) or other RST predictions (Fig. S3) suggest that close to 0°C
 167 permafrost still persists (Fig. S3). At the elevations of Vig_2 and Vig_3, MARST was
 168 close to 0°C during the last period and simulations show that close to 0°C permafrost
 169 subsists down to 30 m depth at Vig_2, independent of the simulation forcing data or ice
 170 content. At Vig_3, close to 0°C temperature goes deeper since the years 2010s.
 171 Permafrost is present at location of Vig_4 (Tab. 2; Fig 3.) but is substantially affected by
 172 the incoming heat flux from the opposite south face, which induces rather warm
 173 permafrost conditions. Without this incoming heat flux, the conditions would likely favor
 174 cold permafrost. (Fig. S3).

		Vig_1	Vig_2	Vig_3	Vig_4
MARST 1961-1990 ($^{\circ}\text{C}$)	Lourdes	-0.5	-1	-1.95	-3.6
	Lourdes -Goriz	-0.4	×	-1.8	-3.35
MARST 1981-2010 ($^{\circ}\text{C}$)	Lourdes	0.03	-0.4	-1.25	-2.8
	Lourdes -Goriz	0.5	×	-0.85	-2.5
MARST 2014-2015	Measurement	×	×	0.21	-1.56

175
 176 **Table 2.** *MARST during two periods and the measurement year 2014-2015.*



177

178

179 **Figure 3.** Bedrock temperature predicted with the best-fitted RST (with the Lourdes-Goriz
 180 regression for Vig_1, Vig_3 and Vig_4 and with the Lourdes regression for Vig_2), with
 181 a 1% porosity value and with a 0.1 W.m^{-1} bottom heat flux for Vig_4.

182 **2.2 Active layer patterns**

183 The active layer thicknesses (ALT) at Vig_3 ($5.5 \pm 1.2 \text{ m}$ depth) and Vig_4 ($3 \pm 0.2 \text{ m}$
 184 depth) during summer 2015 are the only ALT values reported because they were forced
 185 with measured RST. The ice content (porosity value) causes the greater differences in the
 186 active layer thickness value at the relatively warm Vig_3, where latent heat processes
 187 strongly affect the thermal dynamics (Fig. S4).

188 **3 Discussion**

189 Results of this study present the first evidence of rock wall permafrost in the Pyrenees at
 190 42°N . Rock wall permafrost distribution during the period 1961-1990 was similar to that
 191 which was found in north faces of the Mont Blanc massif (45°N) where the lowest
 192 occurrence on the north face was about 2400 m a.s.l. ²¹. ALT in 2015 for Vig_3 and Vig_4
 193 sensors (2983 m a.s.l and 3196 m a.s.l) showed similar values to the Aiguille du Midi site
 194 in the Mont Blanc massif ²⁶.

195 Overall, our results are consistent with the classification described by Serrano et al. ^{6,7}
196 .Our data show that permafrost may subsist at lower elevation (2600 m a.s.l) in fractured
197 areas with higher ice content bedrock (MARST value of -0.5°C) coinciding with the upper
198 limit of the infraperiglacial belt. Currently, close to 0°C permafrost has been identified
199 on the Vignemale North face at 2800 m a.s.l, and up to 3000-3100 m a.s.l (periglacial
200 belt). The upper section of the Vignemale north face, above 3100-3200 m a.s.l, has
201 favorable climate conditions that enable the occurrence of cold ($< -2^{\circ}\text{C}$) permafrost on
202 the north face where no heat flux from a surrounding sun-exposed face significantly
203 warms the subsurface. The main limitations in the interpretation of results are related to
204 the temperature sensor quality ($\pm 0.5^{\circ}\text{C}$), errors in RST reconstruction, which does not
205 account for local and complex meteorological processes, as well as structural and thermal
206 parameters used for thermal modelling.

207 The distribution of permafrost since the 1960s on the rock face has shown profound
208 changes. During the 1961-1990 period, the entire rock face may have been affected by
209 permafrost. By 2010, there was no longer permafrost up to 2600 m a.s.l and close to 0°C
210 permafrost had receded up to 2800 m a.s.l. Since 2010, close to 0°C permafrost has
211 receded to at least 3000 m a.s.l and cold ($< -2^{\circ}\text{C}$) permafrost is only found in shaded areas
212 above 3100 m a.s.l. These results confirm a progressive degradation of permafrost during
213 the last decades as a consequence of increasing air temperatures ¹⁴. Additionally, the rapid
214 wastage and thinning of the Ossoue glacier ¹⁸, could potentially impact the energy balance
215 of the south and east face and increasing the heat flux reaching the north face and
216 intensifying permafrost degradation in the upper sections. The warm character of
217 permafrost ($> -2^{\circ}\text{C}$ up to 3000 m a.s.l) suggests an imminent disappearance of permafrost
218 in the Vignemale, as well as in most of the peaks of the Pyrenees where elevations are
219 lower than 3100 m a.s.l. These findings highlight the need to systematically study rock

220 wall permafrost in the Pyrenees, as this would be an effective baseline for assessing
221 climate change impacts in a relatively low-latitude, but still permafrost-affected mountain
222 range, including hazards assessment, geotechnical and land planning concerns. Land
223 planning in the high elevation areas of the Pyrenees must incorporate the current state of
224 rock wall permafrost state and its future evolution in order to implement mitigation
225 measures.

226 **Conclusions**

227 This study combines RST measurements, meteorological records, statistical analysis, and
228 numerical thermal modelling to provide the first evidence of rock wall permafrost in the
229 Pyrenees at 42 °N and the recent thermal evolution of an emblematic north face wall of
230 the Pyrenees. During the late XX century, permafrost may have affected the entire
231 Vignemale north face (as low as 2600 m a.s.l.) and it has progressively degraded and
232 disappeared as consequence of an increase in air temperature of almost 1.5°C since 1950.
233 The lower limit of close to 0°C permafrost is currently likely between 2800 m a.s.l to
234 3000-3100 m a.s.l, while permafrost may subsist at lower elevations (2600 m a.s.l) in
235 fractured areas with higher ice content bedrock. Climate conditions allow for the
236 occurrence of cold (< -2°C) permafrost above 3100-3200 m a.s.l. but warmer conditions
237 may be found near the top (3298 m a.s.l) due to warm heat fluxes coming from the south
238 face.

239 This study is a preliminary step in demonstrating the interest to more systematically
240 investigate rock wall permafrost in the Pyrenees with the aid of a robust and complete
241 temperature sensor network. More robust monitoring would enable investigations of past
242 and recent thermal dynamics in various topographical settings, permafrost distribution
243 mapping, and determination of potential permafrost evolution in the near future according
244 to available temperature projections.

245 **Acknowledgements**

246 We would like to thank Joserra Vidalier Axpe, Unai García de Olano, Xabier Paternain,
247 and Txomin Bornaetxea for their help during the fieldwork campaigns. We also are
248 grateful to the Parc National des Pyrenees for their support with permits and access to the
249 field site. We thank Sebastian Westermann (University of Oslo, Norway) for providing
250 the CryoGRID model.

251 **References**

- 252 1. Haeberli W, Wegmann M, Mühll D. Slope stability problems related to glacier
253 shrinkage and permafrost degradation in the Alps. *Eclogae Geol Helv.* 1997;90:407-414.
- 254 2. Deline P, Gruber S, Delaloye R, et al. Chapter 15 - Ice Loss and Slope Stability in High-
255 Mountain Regions. In: Shroder JF, Haeberli W, Whiteman Risks and Disasters CBT-S
256 and I-RH, eds. Academic Press; 2015:521-561. doi:[https://doi.org/10.1016/B978-0-12-](https://doi.org/10.1016/B978-0-12-394849-6.00015-9)
257 [394849-6.00015-9](https://doi.org/10.1016/B978-0-12-394849-6.00015-9)
- 258 3. Ravanel L, Magnin F, Deline P. Impacts of the 2003 and 2015 summer heatwaves on
259 permafrost-affected rock-walls in the Mont Blanc massif. *Sci Total Environ.*
260 2017;609:132-143. doi:<https://doi.org/10.1016/j.scitotenv.2017.07.055>
- 261 4. Noetzli J, Gruber S, Kohl T, Salzmann N, Haeberli W. Three-dimensional distribution
262 and evolution of permafrost temperatures in idealized high-mountain topography. *J*
263 *Geophys Res Earth Surf.* 2007;112(F2). doi:10.1029/2006JF000545
- 264 5. Oliva M, Žebre M, Guglielmin M, et al. Permafrost conditions in the Mediterranean
265 region since the Last Glaciation. *Earth-Science Rev.* 2018;185:397-436.
266 doi:<https://doi.org/10.1016/j.earscirev.2018.06.018>
- 267 6. Serrano E, de Sanjosé-Blasco JJ, Gómez-Lende M, López-Moreno JJ, Pisabarro A,
268 Martínez-Fernández A. Periglacial environments and frozen ground in the central

269 Pyrenean high mountain area: Ground thermal regime and distribution of landforms and
270 processes. *Permafrost Periglacial Processes*. 2019;30(4):292-309. doi:10.1002/ppp.2032

271 7. Serrano E, López-Moreno JI, Gómez-Lende M, et al. Frozen ground and periglacial
272 processes relationship in temperate high mountains: a case study at Monte Perdido-
273 Tucarroya area (The Pyrenees, Spain). *J Mt Sci*. 2020;17(5):1013-1031.
274 doi:10.1007/s11629-019-5614-5

275 8. Colucci R, Boccali C, Žebre M, Guglielmin M. Rock glaciers, protalus ramparts and
276 pronival ramparts in the south-eastern Alps. *Geomorphology*. 2016;269.
277 doi:10.1016/j.geomorph.2016.06.039

278 9. Westermann S, Schuler T V, Gislås K, Etzelmüller B. Transient thermal modeling of
279 permafrost conditions in Southern Norway. *Cryosphere*. 2013;7(2):719-739. doi:10.5194/tc-
280 7-719-2013

281 10. Magnin F, Etzelmüller B, Westermann S, Isaksen K, Hilger P, Hermanns R.
282 Permafrost distribution in steep rock slopes in Norway: measurements, statistical
283 modelling and implications for geomorphological processes. *Earth Surf Dyn*.
284 2019;7:1019-1040. doi:10.5194/esurf-7-1019-2019

285 11. Grunewald K, Scheithauer J. Europe's southernmost glaciers: response and adaptation
286 to climate change. *J Glaciol*. 2010;56(195):129-142. doi:10.3189/002214310791190947

287 12. Rico I, Magnin F, López-Moreno JI, Alonso E, Revuelto J, Serrano E. First evidence
288 of permafrost occurrence in a steep rock wall in the Pyrenees: The Vignemale North Face.
289 . In: *VI Iberian Congress of the International Permafrost Association, Mieres (Spain)*. ;
290 2017.

291 13. Desnivel. Diedro amarillo del Vignemale, en cuarentena por derrumbe.
292 [https://www.desnivel.com/escalada-roca/diedro-amarillo-del-vignemale-en-cuarentena-](https://www.desnivel.com/escalada-roca/diedro-amarillo-del-vignemale-en-cuarentena-por-derrumbe)
293 [por-derrumbe](https://www.desnivel.com/escalada-roca/diedro-amarillo-del-vignemale-en-cuarentena-por-derrumbe) Accessed October, 26, 2020 . Published online 2012.

- 294 14. Cuadrat JM, Valero Garcés B, González-Sampériz P, et al. Clima y Variabilidad
295 Climática en los Pirineos. In: Terraez J, Arauzo I, eds. *1º Informe Cambio Climático*
296 *Pirineos OPCC - CTP 2018.* ; 2018:6-16.
- 297 15. Rico I, Izagirre E, Serrano E, López-Moreno J. Superficie glaciaria actual en los
298 Pirineos: Una actualización para 2016. *Pirineos.* 2017;172:029.
299 doi:10.3989/Pirineos.2017.172004
- 300 16. Rico I. Los glaciares de los Pirineos. Estudio glaciológico y dinámica actual en el
301 contexto del cambio global. . Published online 2019.
- 302 17. López-moreno JI, Alonso-González E, Monserrat o, et al. Ground-based remote-
303 sensing techniques for diagnosis of the current state and recent evolution of the Monte
304 Perdido Glacier, Spanish Pyrenees. *J Glaciol.* 2019;65(249):85-100. doi:DOI:
305 10.1017/jog.2018.96
- 306 18. Marti R, Gascoïn S, Houet T, et al. Evolution of Ossoue Glacier (French Pyrenees)
307 since the end of the Little Ice Age. *Cryosph Discuss.* 2015;9:2431-2494. doi:10.5194/tcd-
308 9-2431-2015
- 309 19. López-Moreno JI, Soubeyroux J-M, Gascoïn S, et al. Long-term trends (1958–2017)
310 in snow cover duration and depth in the Pyrenees. *Int J Climatol.* Published online March
311 29, 2020. doi:10.1002/joc.6571
- 312 20. Navarro-Serrano F, López-Moreno JI, Azorin-Molina C, et al. Air temperature
313 measurements using autonomous self-recording dataloggers in mountainous and snow
314 covered areas. *Atmos Res.* 2019;224:168-179.
315 doi:https://doi.org/10.1016/j.atmosres.2019.03.034
- 316 21. Magnin F, Brenning A, Bodin X, Deline P, Ravanel L. Statistical modelling of rock
317 wall permafrost distribution: Application to the Mont Blanc massif. *Géomorphologie.*
318 Published online January 1, 2015.

319 22. Westermann S, Schuler T V, Gislås K, Eitzelmüller B. Transient thermal modeling of
320 permafrost conditions in Southern Norway. *Cryosph.* 2013;7(2):719-739. doi:10.5194/tc-
321 7-719-2013

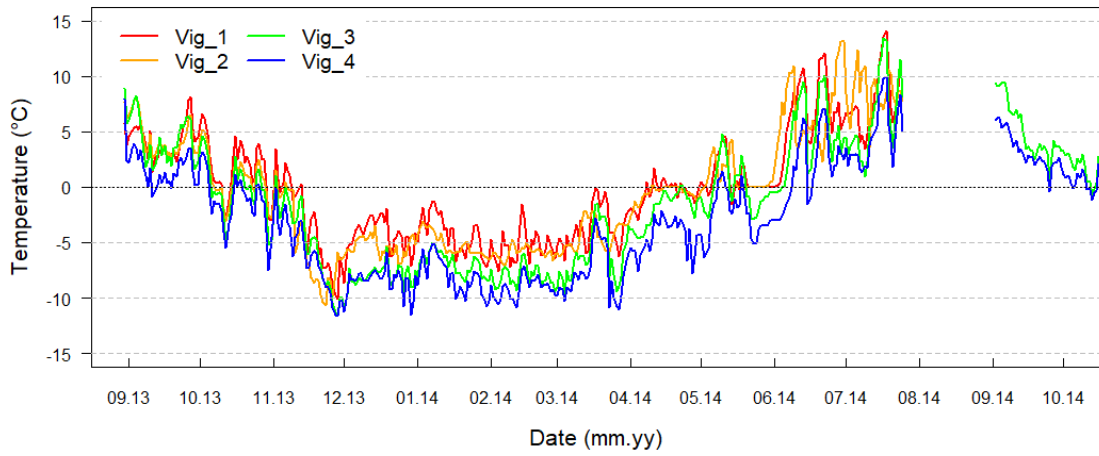
322 23. Kukkonen IT, Šafanda J. Numerical modelling of permafrost in bedrock in northern
323 Fennoscandia during the Holocene. *Glob Planet Change.* 2001;29(3):259-273.
324 doi:[https://doi.org/10.1016/S0921-8181\(01\)00094-7](https://doi.org/10.1016/S0921-8181(01)00094-7)

325 24. Magnin F, Westermann S, Pogliotti P, Ravanel L, Deline P, Malet E. Snow control
326 on active layer thickness in steep alpine rock walls (Aiguille du Midi, 3842ma.s.l., Mont
327 Blanc massif). *CATENA.* 2017;149:648-662.
328 doi:<https://doi.org/10.1016/j.catena.2016.06.006>

329 25. Beutel J, Delaloye R, Hilbich C, et al. *PERMOS 2019. Permafrost in Switzerland*
330 *2014/2015 to 2017/2018.* Vol 16-19. (Nötzli J, Pellet C, Staub B, eds.). Cryospheric
331 Commission of the Swiss Academy of Sciences (SCNAT); 2019. doi:10.13093/permos-
332 rep-2019-16-19

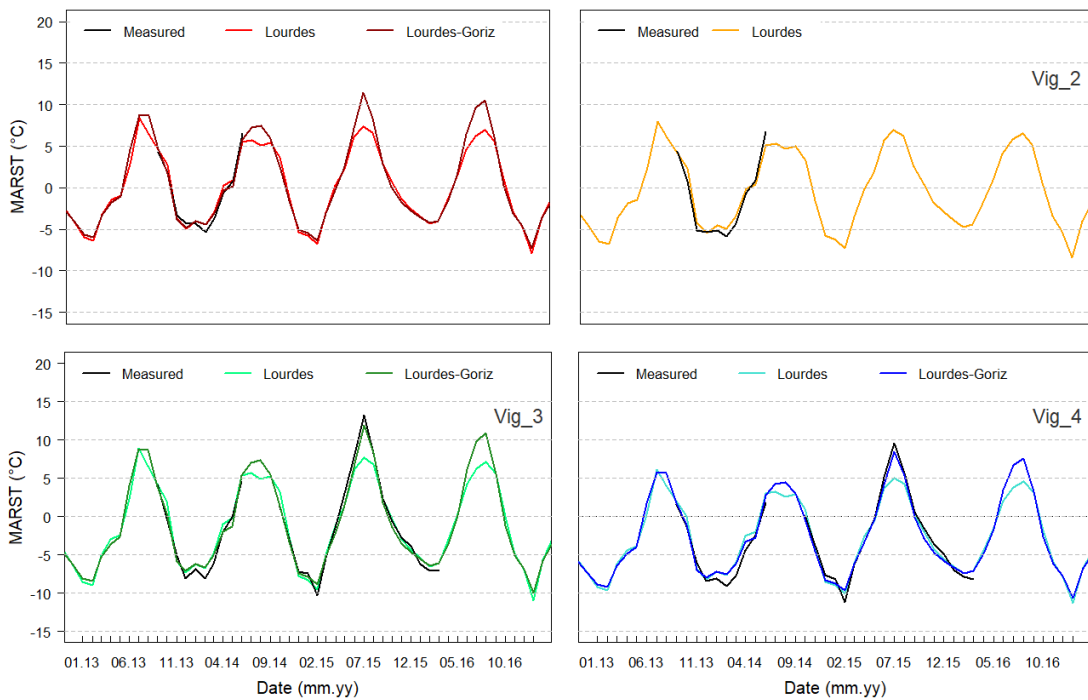
333 26. Magnin F, Deline P, Ravanel L, Noetzli J, Pogliotti P. Thermal characteristics of
334 permafrost in the steep alpine rock walls of the Aiguille du Midi (Mont Blanc Massif,
335 3842 m a.s.l). *Cryosph.* 2015;9(1):109-121. doi:10.5194/tc-9-109-2015
336
337
338
339
340
341
342
343
344
345
346

347 **Supplement**



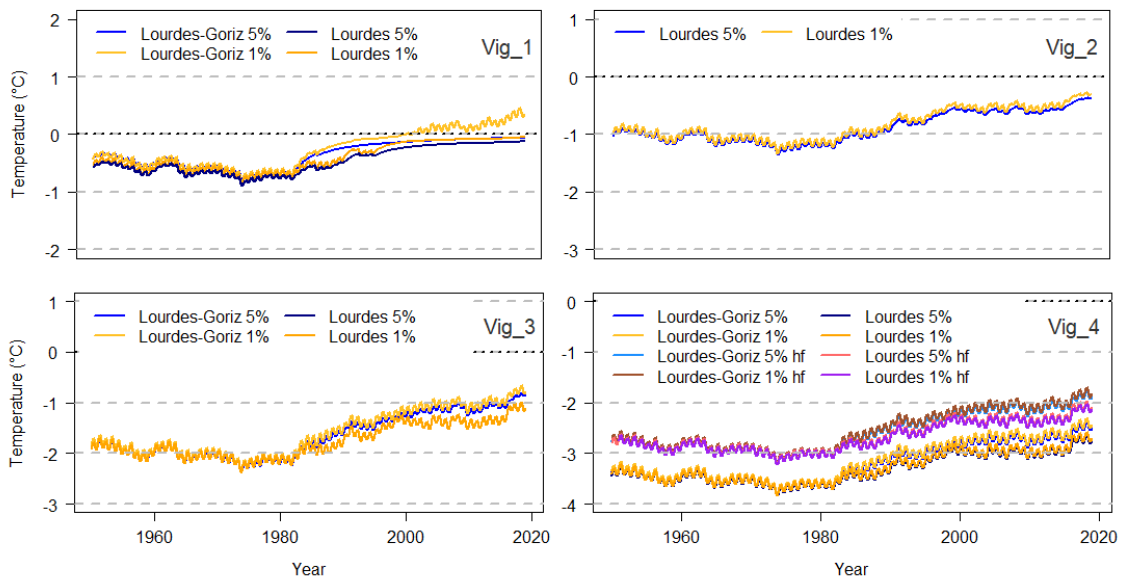
348

349 **Figure S1.** Measured rock surface temperature time series aggregated in daily values



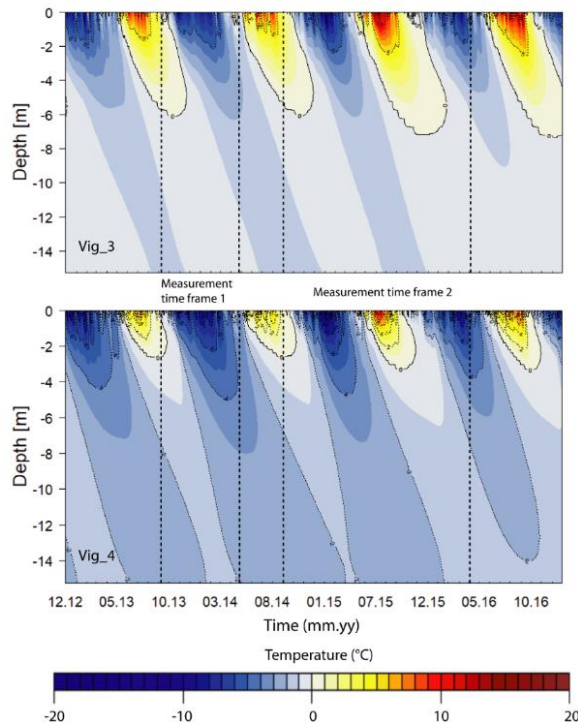
350

351 **Figure S2.** Measured against predicted RST time series (monthly means). « Lourdes » is
352 the linear regression fitted with all daily values of RST while « Lourdes-Goriz » are times
353 series combining a linear regression with Lourdes data from mid-September to mid-May
354 and a regression with Goriz from mid-May to mid-September.



355

356 **Figure S3:** Modelled temperature at 15 m depth of each logger according to the various
 357 regressions and porosity value (5 and 1%) as well as without or with heat flux (hf).



358

359 **Figure S4.** Focus on active layer thickness during years of RST measurements at Vig_3
 360 and Vig_4.

361

	Vig_3	Vig_4
Measured (2014-2015)	0.21	-1.56
Lourdes regression	-0.5	-2.2
Lourdes-Goriz regression	-0.17	-1.9

362 **Table S1.** Comparison between measured and predicted mean annual RST for the
363 hydrological year 2014-2015.

		Vig_1	Vig_2	Vig_3	Vig_4
All year	R²	0.86	0.76	0.85	0.85
Lourdes	Regression	0.8274x – 10.38	0.8314x – 10.875	1.0041x – 13.888	0.8837x – 13.962
	Obs. pts*	332	332	942	942
Winter	R²	0.84	0.75	0.81	0.80
Lourdes	Regression	0.7072x – 9.4018	0.6608x – 9.7221	0.8097x – 12.383	0.7396x – 12.85
	Obs. pts*	242	242	683	683
Summer	R²	0.75	0.32	0.88	0.83
Goriz	Regression	0.8621x – 2.5535	0.5595x + 0.6494	1.0053 – 4.4072	0.8635x – 5.5722
	Obs. pts*	90	90	266	266

364 **Table S2.** Regression values between RST and AT. *Obs. pts is the number of available
365 daily RST measurements for regression calibration.

		Vig_1		Vig_2		Vig_3		Vig_4	
		Lourdes	L-G	Lourdes	L-G	Lourdes	L-G	Lourdes	L-G
MARST difference between measure and prediction		×	×	×	×	0.71	0.38	0.64	0.34
R²	Month	0.97	0.98	0.96	×	0.95	0.98	0.94	0.97
	Day	0.86	0.9	0.76	×	0.85	0.92	0.85	0.9
Mean error (°C)	Month	0.19	0.02	0.29	×	0.39	0.33	0.9	0.58
	Day	0	- 0.02	0	×	0	- 0.03	0	- 0.02
Standard deviation (°C)	Month	0.7	0.57	0.94	×	0.6	0.86	0.79	0.78
	Day	1.8	1.6	2.58	×	2.48	1.83	2.19	1.74

366 **Table S3.** Summary of predicted RST errors.